Struct Chem (2011) 22:1233–1240
DOI 10.1007/s11224-011-9816-x

ORIGINAL RESEARCH

Synthesis, characterization, crystal structure and cytotoxicity of 2,4-bis(selenomethyl)quinazoline

Daniel Plano · Elena Ibáñez · Juan Antonio Palop · Carmen Sanmartín

Received: 18 January 2011 / Accepted: 31 May 2011 / Published online: 17 June 2011
© Springer Science+Business Media, LLC 2011

Abstract Organoselenium compounds have already been reported to be good anticarcinogenic candidates. A new selenoquinazoline derivative, 2,4-bis(selenomethyl)quinazoline (compound **1**), has been synthesized, spectroscopically characterized and its crystal structure has been studied. An intermolecular coupling between C_2 and H'_5 in the Heteronuclear Multiple Bond Correlation (HMBC) experiment has been observed. Assuming that the head-to-tail overlap of parallel molecules (as identified by X-ray diffraction) remains in solution to give bimolecular entities, the π–π interaction enables heteronuclear coupling between the former atoms with a three-bond distance [$C_2\cdots(\pi\text{–}\pi)\cdots C'_5\text{–}H'_5$]. The crystal structure of compound **1** has been solved by X-ray diffraction. It crystallizes in triclinic system, space group $P-1$. Unit cell parameters are $a = 7.4969(7)$ Å, $b = 8.7008(8)$ Å, $c = 10.1666(9)$ Å, $\alpha = 110.215(2)°$, $\beta = 90.354(2)°$, $\gamma = 115.017(1)°$. Linear chains in crystals of compound **1** are generated by C–H···Se and Se···Se bonds between molecules. Furthermore, head-to-tail overlap of parallel molecules, in which π–π interactions can occur, is observed. Compound **1** exhibited a cytotoxic effect in all of the evaluated tumoral cell lines and showed a higher cytotoxic effect in colon and breast cancer cell lines than etoposide, which was used as a reference compound.

Keywords Selenium · Synthesis · Spectroscopic characterization · Crystal structure · X-ray diffraction · Cytotoxicity

D. Plano (✉) · E. Ibáñez · J. A. Palop · C. Sanmartín
Department of Organic and Pharmaceutical Chemistry, University of Navarra, Irunlarrea, 1, 31008 Pamplona, Spain
e-mail: dplano@alumni.unav.es

Introduction

Selenium (Se) is an essential trace element that is involved in different physiological functions in the human body. Epidemiological and clinical studies indicate that inadequate levels of selenium increase the risk of cancer and nutritional intervention studies show that high Se intakes effectively reduce mammary, prostate, lung, colon and liver cancer risk [1–5]. Basic research and clinical trials strongly support the protective role of selenium against various types of cancer. This effect was more remarkable in prostate and colorectal cancers [6–8]. A recent report from the Selenium and Vitamin E Cancer Prevention Trial (SELECT) demonstrated that selenium or vitamin E, either alone or in combination did not prevent prostate cancer or secondary cancers [9]. However, the failure of one form of Se does not disprove the possible protective effect of other forms of Se. In fact, the anticancer activity of Se is dependent on its chemical form and dosage. The results of the SELECT caused much controversy, the formulation of Se used (selenomethionine) being one of the topics discussed [10]. Selenomethionine can be incorporated non-specifically into proteins in place of methionine [11]. Compartmentation into tissue proteins limits selenomethionine from being further metabolized.

The mechanisms of action for Se and selenocompounds as anticancer agents are not fully understood. However, it has been proposed in the literature that antioxidant properties [12], cell cycle modulation [13, 14], apoptosis induction [15, 16] and angiogenesis inhibition [17, 18] may be some of the possible molecular targets for Se compounds.

One of our ongoing research projects involves the investigation of novel potential antitumor and leishmanicidal agents containing at least one selenium atom [19–24].

Our research group has synthesized a series of imidoselenocarbamates, some of which show better in vitro antitumor effects than certain chemotherapeutic agents (including etoposide, taxol and methotrexate) in several cell lines [19, 20]. These derivatives also showed antileishmanial activity in vitro against *Leishmania infantum* [21]. Our research group also prepared and evaluated a series of selenylacetic acids [22], selenocyanates and diselenides derivatives [23], and selenadiazoles [24].

The work described here involved the synthesis and cytotoxicity evaluation of 2,4-bis(selenomethyl)quinazoline (**1**) in four human tumour cell lines (CCRF-CEM, HTB54, HT-29 and MCF-7) and one non-malignant mammary gland-derived cell line (184B5). In addition, we present the molecular characterization and the X-ray crystal structure determination for this compound.

Experimental

Synthesis and characterization

Melting points were determined with a Mettler FP82 + FP80 apparatus (Greifense, Switzerland) and are uncorrected. The ^{1}H-NMR spectra were recorded on a Bruker 400 Ultrashield™ spectrometer (Rheinstetten, Germany) using TMS as the internal standard. The IR spectra were obtained on a Thermo Nicolet FT-IR Nexus spectrophotometer with KBr pellets. Elemental microanalyses were carried out on vacuum-dried samples using a LECO CHN-900 Elemental Analyzer. Alugram® SIL G/UV254 (Layer: 0.2 mm) (Macherey–Nagel GmbH & Co. KG. Postfach 101352, 52313 Düren, Germany) was used for Thin Layer Chromatography. Chemicals were purchased from E. Merck (Darmstadt, Germany), Scharlau (F.E.R.O.S.A., Barcelona, Spain), Panreac Química S.A. (Montcada i Reixac, Barcelona, Spain), Sigma-Aldrich Química S.A. (Alcobendas, Madrid, Spain), Acros Organics (Janssen Pharmaceuticalaan 3a, 2440 Geel, België) and Lancaster (Bischheim-Strasbourg, France).

Chemical preparation

The synthetic route for 2,4-bis(selenomethyl)quinazoline (**1**) is depicted in Fig. 1.

Synthesis of 2,4-dichloroquinazoline

A mixture of 2,4(1*H*,3*H*)-quinazolinedione [2.00 g; 12.3 mmol] in a large excess of phosphoryl chloride [10 mL] and *N*,*N*-dimethylaniline [1.6 mL; 12.5 mmol] was heated under reflux for 14 h. The mixture was poured onto ice [200 g] and the resulting solid was filtered off, washed with distilled water and dried. This compound was used without further purification.

Synthesis of quinazoline-2,4-diselenol hydrochloride

Selenourea [1.25 g; 10.2 mmol] was added to a solution of 2,4-dichloroquinazoline [1.85 g; 9.3 mmol] in absolute ethanol [50 mL] and the reaction mixture was heated under reflux for 2 h. The resulting solid was filtered off while warm and washed with distilled water and cold ethanol [3 × 25 mL]. The desired compound was obtained and used without further purification.

$M = 288.07$ g mol^{-1}. Yield: 83%. m.p. 228.7 ± 1.4 °C. IR (KBr pellet, cm^{-1}): 1610 [ν(C_2=N)], 1552 [ν(C_4=N)]. ^{1}H-NMR (400 MHz, DMSO-d_6) (δ/ppm): 7.34–7.41 (m, 2H, $H_5 + H_7$); 7.85 (t, 1H, $J_{6\text{-}7} = J_{6\text{-}5} = 7.7$ Hz, H_6); 8.30 (t, 1H, $J_{8\text{-}7} = 8.2$ Hz, H_8); 13.84 (bs, 2H, 2SeH). Anal Calcd. for $C_8H_6N_2Se_2$ (0.5 HCl): C 31.34, H 2.12, N 9.14. Found: C 31.20, H 1.96, N 9.15.

Synthesis of 2,4-bis(selenomethyl)quinazoline (**1**)

Iodomethane [1.57 mL; 25.2 mmol] was added to a solution of quinazoline-2,4-diselenol hydrochloride [2.57 g; 8.4 mmol] in 0.4 N NaOH [20 mL]. The mixture was stirred at room temperature for 1 h. The resulting solid was filtered off, washed with distilled water and recrystallized from ethanol.

$M = 316.12$ g mol^{-1}. Yield: 80%. m.p. 61.4 ± 0.8 °C. IR (KBr pellet, cm^{-1}): 1608 [ν(C_2=N)], 1552 [ν(C_4=N)]. ^{1}H-NMR (400 MHz, DMSO-d_6) (δ/ppm): 2.53 (s, 3H, Se_{41}–CH_3); 2.56 (s, 3H, Se_{21}–CH_3); 7.61 (ddd, 1H, $J_{6\text{-}5} = 8.2$ Hz, $J_{6\text{-}7} = 7.0$ Hz, $J_{6\text{-}8} = 1.2$ Hz, H_6); 7.77 (dd, 1H, $J_{8\text{-}7} = 8.4$ Hz, H_8); 7.92 (ddd, 1H, $J_{7\text{-}5} = 1.2$ Hz, H_7); 7.95 (dd, 1H, H_5). ^{13}C-NMR (100 MHz, DMSO-d_6) (δ/ppm): 6.7 (Se_{41}–CH_3); 7.6 (Se_{21}–CH_3); 124.2 (C_{10}); 126.1 (C_5); 127.8 ($C_6 + C_8$); 135.7 (C_7); 148.7 (C_9); 164.6 (C_4); 171.8 (C_2). Anal Calcd. for $C_{10}H_{10}N_2Se_2$: C 37.97, H 3.16, N 8.86. Found: C 37.86, H 3.03, N 8.72.

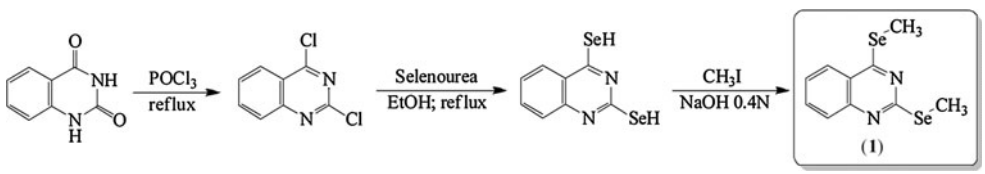

Fig. 1 Synthetic route for preparation of 2,4-bis(selenomethyl)quinazoline (**1**)

X-ray structure determination

Intensity data were collected on a Bruker SMART-APEX automatic X-ray diffractometer with a CCD area detector using graphite-monochromated Mo K_α radiation ($\lambda = 0.71073$ Å). A trial data collection revealed that the selected crystal was of high quality and this permitted the measurement of preliminary unit cell parameters. The structure determination was carried out by collecting diffracted intensities through 1365 exposures/scans with 10 s/exposure to scan in Ewald half-sphere at least 25° of θ completely. Absorption corrections (program SADABS [25]) were applied to the intensity data. SHELXTL-NT 6.1 [26] was employed to solve and refine the crystal structure. The structure was refined by the least-squares method on F^2 using all reflections. The non-hydrogen atoms were refined with anisotropic displacement factors. The positions of hydrogen atoms were calculated considering the nature of the atom that they are linked to. The (x,y,z) coordinates of these hydrogens were refined jointly with the atoms to which they are bonded and isotropic displacement parameters set at 1.5 times (methylic hydrogens) or 1.2 times (benzylic hydrogens) the U_{eq} of the parent atoms were used.

The space group determination is not unequivocal, since for a triclinic lattice two space groups are possible: $P1$ and $P-1$. Space group $P-1$ seems to be more probable according to the distribution of intensities and other statistical parameters. The resolution was carried out by direct methods. All non-hydrogen atoms in the molecule were found using an E-map prepared from the set of stages with the best figure of merit, which has confirmed the space group.

Cytotoxicity

The cytotoxic effect of compound **1** was tested at five different concentrations between 0.01 and 100 μM. Compound **1** was initially dissolved in DMSO at a concentration of 0.1 M and serial dilutions were prepared using culture medium. The plates with cells from the different lines, to which medium containing the substance under test was added, were incubated for 72 h at 37 °C in a humidified atmosphere containing 5% CO_2. Human tumour cell lines were provided by the European Collection of Cell Cultures (ECACC) or the American Type Culture Collection (ATCC). Five cell lines were used: one human lymphocytic leukaemia (CCRF-CEM), three human solid tumours, one colon carcinoma (HT-29), one lung carcinoma (HTB-54), one breast adenocarcinoma (MCF-7) and one non-tumoral cell line (184B5). CCRF-CEM, HT-29 and HTB-54 cells were grown in RPMI 1640 medium (Invitrogen) supplemented with 10% foetal calf serum, 2 mM L-glutamine, 100 units/mL penicillin, 100 μg/mL streptomycin and 10 mM HEPES buffer (pH 7.4). MCF-7 cells were grown in EMEM medium (Clonetics) supplemented with 10% foetal calf serum, 2 mM L-glutamine, 100 units/mL penicillin and 100 μg/mL streptomycin. 184B5 cells were grown in Hams F-12/DMEM (50:50) supplemented as described in the literature [27]. Cytotoxicity was then determined by the MTT method. Results are expressed as GI_{50}, the concentration that reduces by 50% the growth of treated cells with respect to untreated controls, TGI, the concentration that completely inhibits cell growth, and LC_{50}, the concentration that kills 50% of the cells. Data were obtained from at least 3 independent experiments performed in quadruplicate.

Results and discussion

Molecular characterization

The ν(C=N) of the quinazoline moiety in the IR spectrum can be assigned to bands at 1608 and 1552 cm^{-1}. The first of these bands could correspond to a C_2=N bond because C_2 supports a higher positive charge density than C_4 since it is located between two nitrogen atoms. Therefore, a stronger bond exists for the C_2 atom and the corresponding band will appear at higher wavenumber than that for C_4.

The structure of compound **1** could not be unequivocally assigned by monodimensional NMR experiments and a bidimensional experiment was therefore carried out. The aims of the HMBC experiment were twofold: (a) the correct assignment of the signals for the methyl groups attached to the selenium atoms in the ^{1}H-NMR spectrum; and (b) the unequivocal assignment of the signals of the aromatic carbon atoms in the ^{13}C-NMR spectrum.

It can be seen from the HMBC spectrum shown in Fig. 2 that there is heteronuclear coupling between the protons of the methyl group attached to Se_{21} and the C_2 atom (2.56–171.8 ppm). The same coupling appears between the protons of the methyl group attached to Se_{41} and the C_4 atom (2.53–164.6 ppm). The assignment of the aromatic carbon signals was made based on the coupling observed with the aromatic hydrogen signals. Furthermore, an unexpected coupling between H_5 and C_2 (7.95–171.8 ppm) was observed. This signal might not correspond to an intramolecular coupling due to the five-bond distance between these two atoms. A possible explanation for this observation was investigated by single crystal X-ray diffraction.

Crystal characterization

The crystal data and refinement details for compound **1** are listed in Table 1. The optimization of the unit cell

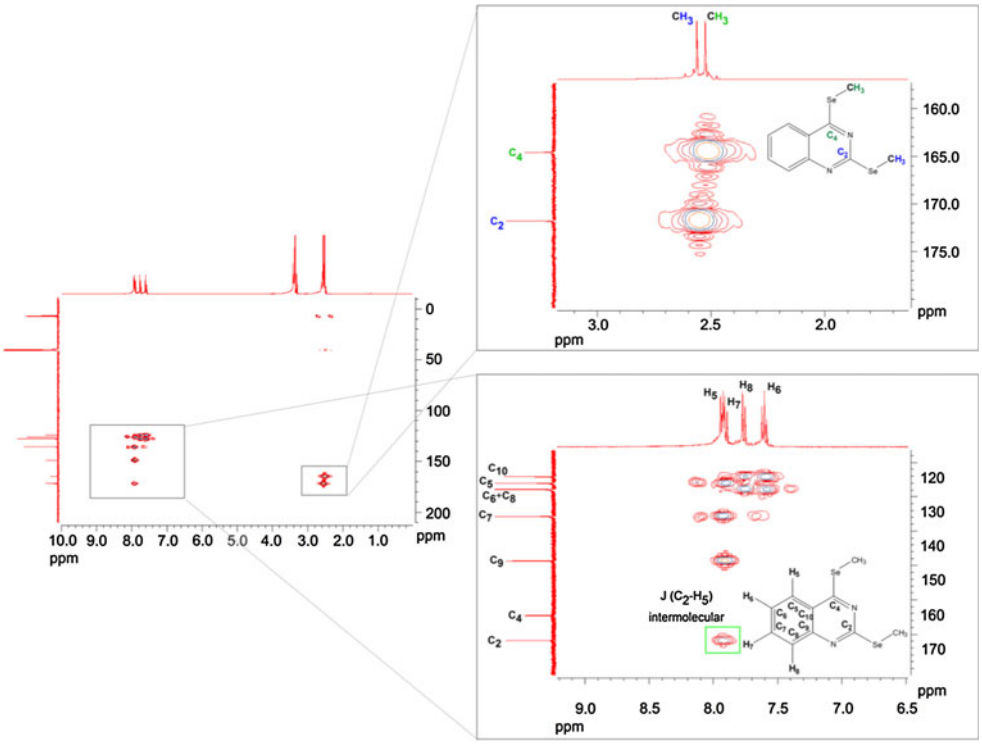

Fig. 2 HMBC spectrum of compound **1**

parameters was performed by least-squares refinement of the angular positions of the 1692 reflections in the range from 2.80° to 27.69° (θ). These parameters correspond to a triclinic lattice. The adjustment by a least-squares method of the angular positions of 1674 reflections in the range from 2.81° to 27.61° (θ) considering the cell as pseudomonoclinic led to the following parameters: $a = 15.7692(14)$ Å, $b = 7.4969(7)$ Å, $c = 10.1652(10)$ Å, $\beta = 112.593(2)°$ and the α and γ parameters deviated significantly from 90°: 90.326(2)° and 89.524(2)°, respectively. Nevertheless, analysis of the equivalent reflections, considering the crystal as monoclinic, revealed an R_{int} value of 0.54, which indicates that the cell is not monoclinic.

A representation of the molecular structure based on the X-ray analysis, showing thermal ellipsoids is shown in Fig. 3. Table 2 includes geometric parameters of compound **1**.

The direction of the C_4–Se_{41} bond coincides with the corresponding cyclic angle bisector, N_3–C_4–C_{10}, while the position of the C_2–Se_{21} bond is slightly asymmetric, distanced from the other substituent [exocyclic angles of 113.6° and 117.5(2)°] (Table 2).

The quinazoline unit is almost flat and the largest deviation from the plane defined by the ten atoms is 0.012(3) Å. The two substituents are located practically in the mean plane of the quinazoline unit with the methyl groups close to it (i.e. forming the shape of a clamp, Fig. 3).

Evidence for weak intermolecular hydrogen bonds C_{ar}–H···Se is observed in the crystal structure:

C_6–H_6, 0.93 Å; C_6···Se_{21}(i), 3.866(5) Å; H_6···Se_{21}(i), 3.05 Å; C_6–H_6···Se_{21}(i), 147° [(i): $x, y, z + 1$].

C_8–H_8, 0.93 Å; C_8···Se_{41}(i), 3.998(5) Å; H_8···Se_{41}(i), 3.14 Å; C_8–H_8···Se_{41}(i), 155° [(i): $x, y, z + 1$]

The first such bond leads to infinite molecular chains in the [010] direction (Fig. 4a). On the other hand, there are Se···Se contacts [Se_{41}···$Se_{41}(-x + 1, -y + 1, -z + 1)$] with a distance, 3.7399(6) Å, that is shorter than the sum of the van der Waals radii, 3.80 Å (Fig. 4b).

Moreover, head-to-tail overlap of parallel molecules, in which π–π interactions can occur, is observed (Fig. 5a). The distance between the molecular planes is 3.5 Å and the normal component to these planes shows an angle of 23° with the stacking direction. Data show that the distance between the pyrimidine ring centroids and the distance between the benzene centroid and the pyrimidine centroid of adjacent molecules in the stack is almost the same, 3.814(2) Å, while the distance between the benzene centroids is 5.102(2) Å (Fig. 5b).

Considering the arrangement of the two molecules in a stack (Fig. 5b), a possible explanation for the coupling between H_5 and C_2 seen in the HMBC experiment (Fig. 2) can be proposed. Assuming that the head-to-tail overlap of parallel molecules remains in solution to give bimolecular entities, the π–π interaction enables the heteronuclear coupling between the former atoms with a three-bond

Table 1 Crystal data and refinement details for compound **1**

Empirical formula	$C_{10}H_{10}N_2Se_2$
Formula weight	316.12
Temperature (K)	294(2)
Wavelength (Å)	0.71073
Crystal system, space group	Triclinic, $P-1$
Unit cell dimensions	
a (Å)	7.4969(7)
b (Å)	8.7008(8)
c (Å)	10.1666(9)
α (°)	110.215(2)
β (°)	90.354(2)
γ (°)	115.017(1)
V (Å^3)	554.81(9)
Z, Calculated density (g cm^{-3})	2, 1.892
Absorption coefficient (mm^{-1})	6.626
F(0 0 0)	304
Crystal size (mm^3)	0.40 × 0.19 × 0.06
θ range for data collection (°)	2.17–28.77
Limiting Miller index	$-9 \le h \le 10$
	$-9 \le k \le 11$
	$-13 \le l \le\le 7$
Collected/unique reflections	3817/2568 [$R_{int} = 0.0120$]
Observed reflections [$I > 2\sigma(I)$]	2143
Absorption correction	Semiempirical
Max. and min. transmission	0.672 and 0.083
Refinement method	Full-matrix least-squares on F^2
Data/restraints/parameters	2568/0/129
Goodness-of-fit on F^2	1.035
Final R	$R_1 = 0.0365$, $wR_2 = 0.0941$
R (all data)	$R_1 = 0.0449$, $wR_2 = 0.0988$
Max/min electron density (e Å^{-3})	1.000/−0.449

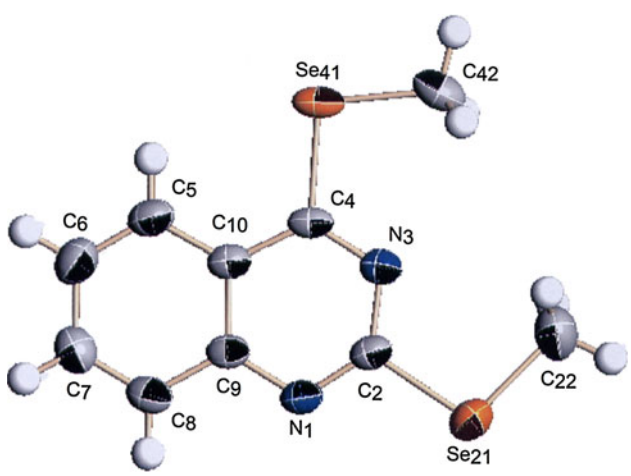

Fig. 3 A representation of the molecular structure based on the X-ray analysis, showing thermal ellipsoids

Table 2 Geometric parameters (Å, °) for compound **1**

Parameter	Compound **1**
Bond lengths (Å)	
N(1)–C(2)	1.304(4)
N(1)–C(9)	1.367(4)
C(2)–N(3)	1.356(3)
C(2)–Se(21)	1.903(3)
N(3)–C(4)	1.313(4)
C(4)–C(10)	1.421(4)
C(4)–Se(41)	1.898(2)
C(5)–C(6)	1.360(5)
C(5)–C(10)	1.408(5)
C(6)–C(7)	1.398(5)
C(7)–C(8)	1.361(5)
C(8)–C(9)	1.409(4)
C(9)–C(10)	1.418(4)
Se(21)–C(22)	1.918(4)
Se(41)–C(42)	1.919(4)
Bond angles (°)	
C(2)–N(1)–C(9)	115.7(2)
N(1)–C(2)–N(3)	128.9(3)
N(1)–C(2)–Se(21)	113.6(2)
N(3)–C(2)–Se(21)	117.5(2)
C(4)–N(3)–C(2)	115.7(3)
N(3)–C(4)–C(10)	122.6(2)
N(3)–C(4)–Se(41)	118.5(2)
C(10)–C(4)–Se(41)	118.9(2)
C(6)–C(5)–C(10)	120.7(3)
C(5)–C(6)–C(7)	120.4(3)
C(8)–C(7)–C(6)	120.9(3)
C(7)–C(8)–C(9)	120.0(3)
N(1)–C(9)–C(8)	119.5(3)
N(1)–C(9)–C(10)	121.2(3)
C(8)–C(9)–C(10)	119.4(3)
C(5)–C(10)–C(9)	118.6(3)
C(5)–C(10)–C(4)	125.4(3)
C(9)–C(10)–C(4)	115.9(3)
C(2)–Se(21)–C(22)	100.51(16)
C(4)–Se(41)–C(42)	98.83(14)

distance [$C_2 \cdots (\pi\text{–}\pi) \cdots C_5'\text{–}H_5'$]. Therefore, the highlighted signal in Fig. 2 might correspond to an intermolecular coupling in the bimolecular entities in solution.

Cytotoxic activity

The newly synthesized compound **1** was evaluated for its in vitro cytotoxic activity against CCRF-CEM (lymphocytic leukaemia), HTB-54 (lung carcinoma), HT-29 (colon

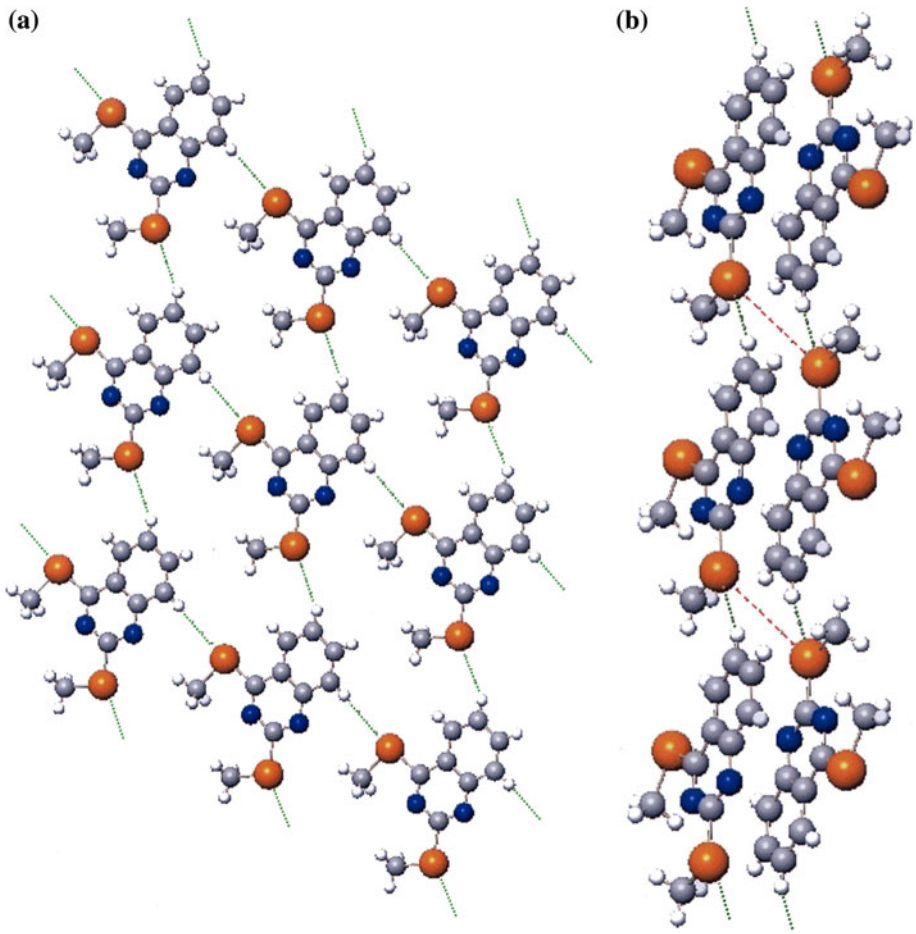

Fig. 4 Linear chains in crystals of compound **1** generated by C–H···Se and Se···Se bonds between molecules. **a** Parallel planes to (100) consisting of molecules joined by C–H···Se hydrogen bonds. **b** Chains parallel to direction [001]. The Se···Se are less than 3.80 Å (sum of the van der Waals radii) and are indicated

carcinoma) and MCF-7 (breast adenocarcinoma), as well as 184B5 (non-malignant cells derived from mammary gland). The cytotoxic activity was determined by the MTT assay [28], after exposure of cells to the compound **1** for 72 h. The results are presented in Table 3.

Compound **1** exhibited a cytotoxic effect in all of the evaluated tumoral cell lines. The most sensitive cell lines to compound **1** were HT-29 and MCF-7. Moreover, the test compound showed good selectivity in these two cell lines against 184B5, presenting GI_{50} values tenfold lower for tumoral cells. 2,4-Bis(selenomethyl)quinazoline (**1**) showed a stronger cytotoxic effect than etoposide, which was used as a reference compound, in HT-29 and MCF-7.

Conclusions

A new selenoquinazoline derivative [2,4-bis(selenomethyl)quinazoline] has been synthesized, structurally characterized and biologically evaluated. The structure of the new compound was assigned by elemental analysis, IR spectroscopy and mono- and bidimensional NMR spectroscopy. The crystal structure was solved by X-ray diffraction. Head-to-tail overlap of parallel molecules in which π-π interactions can occur, and C–H···Se and Se···Se bonds between adjacent molecules allow a linear chain arrangement in the lattice of compound **1**. This derivative showed a cytotoxic effect in all of the evaluated tumoral cell lines. Two cancer cells (HT-29 and MCF-7) proved to be the most sensitive to compound **1**, with stronger antitumoral activity than etoposide (reference compound) observed in these cell lines. Considering its biological profile (cytotoxicity and selectivity), compound **1** emerges as a new lead compound for further testing with the aim of finding more selective and active anticancer drugs.

Supplementary data

CCDC 808487 contains the supplementary crystallographic data for this paper. These data can be obtained free of charge from http://www.ccdc.cam.ac.uk/data_request/cif, by emailing data_request@ccdc.cam.ac.uk, or by contacting The Cambridge Crystallographic Data Centre, 12, Union Road, Cambridge CB2 1EZ, UK; fax: +44-1223-336033.

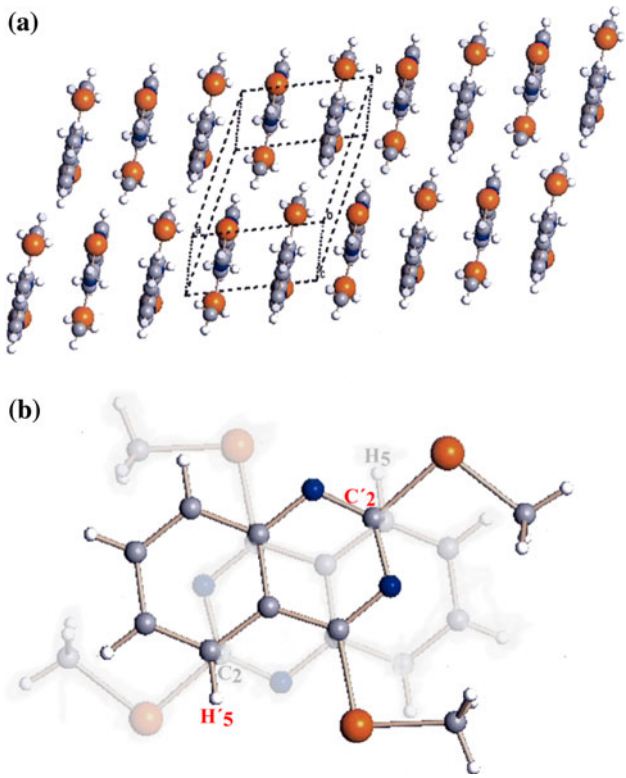

Fig. 5 Crystal packing diagrams for compound **1**. **a** Stacking of parallel molecules showing the unit cell. **b** Overlap of two adjacent molecules in a stack

Table 3 In vitro cytotoxicity of compound **1** determined by MTT assay at 72 h

Compound	Cytotoxic parameters (μM)	Cell lines				
		CCRF-CEM[a]	HTB-54[b]	HT-29[c]	MCF-7[d]	184B5[e]
1	GI_{50}^{f}	31.22	26.55	7.46	5.97	71.48
	TGI[g]	54.85	84.24	33.76	50.73	>100
	LD_{50}^{h}	78.48	>100	76.78	>100	>100
Etoposide[i]	GI_{50}	12.59	nd[j]	31.62	19.95	nd
	TGI	>100	nd	>100	>100	nd
	LD_{50}	>100	nd	>100	>100	nd

[a] Leukemia, [b] Lung carcinoma, [c] Colon carcinoma, [d] Breast adenocarcinoma, [e] Nontumorigenic breast epithelial cells, [f] Concentration that inhibits 50% of cell growth, [g] Concentration that inhibits 100% of cell growth, [h] Concentration that kills 50% of cells, [i] NCI data (http://dtp.nci.nih.gov), [j] No data

Acknowledgments The authors wish to express their gratitude to the Ministerio de Educación y Ciencia, Spain (SAF 2009-07744) for financial support. We also thank the Department of Education of the Navarra Government for the award of a grant (E.I.). The authors would like to thank Dr Rafael Sirera, Department of Chemistry and Soil Science, University of Navarra, for helpful discussions of the results of X-ray diffraction. Many thanks to Dr Ángel Álvarez, X-ray diffraction service, Universitat Autònoma de Barcelona, for X-ray experimental assistance.

References

1. Pan MH, Ho CT (2008) Chemopreventive effects of natural dietary compounds on cancer development. Chem Soc Rev 37:2558–2574
2. Clark LC, Combs GF Jr, Turnbull BW, Slate EH, Chalker DK, Chow J, Davis LS, Glover RA, Graham GF, Gross EG, Krongrad A, Lesher JL Jr, Park HK, Sanders BB Jr, Smith CL, Taylor JR (1996) Effects of selenium supplementation for cancer prevention in patients with carcinoma of the skin. A randomized controlled trial. Nutritional Prevention of Cancer Study Group. JAMA 276:1957–1963
3. Okuno T, Shimamura Y, Mizuno M, Miyata S, Miyake T, Itokawa Y, Takada J, Matsushita R, Koyama M (1988) Trace elements in hepatoma tissue. Trace Elem Med 5:130–136
4. Boosalis MG (2008) The role of selenium in chronic disease. Nutr Clin Pract 23:152–160
5. Araldi EMV, Dell'Aica I, Sogno I, Lorusso G, Garbisa S, Albini A (2008) Natural and synthetic agents targeting inflammation and angiogenesis for chemoprevention of prostate cancer. Curr Cancer Drug Target 8:146–155
6. Zeng H, Combs GF Jr (2007) Selenium as an anticancer nutrient: roles in cell proliferation and tumor cell invasion. J Nutr Biochem 19:1–7
7. Facompre N, El-Bayoumy K (2009) Potential stages for prostate cancer prevention with selenium: implications for cancer survivors. Cancer Res 69:2699–2703
8. Peters U, Takata Y (2008) Selenium and the prevention of prostate and colorectal cancer. Mol Nutr Food Res 52:1261–1272
9. Lippman SM, Klein EA, Goodman PJ, Lucia MS, Thompson IM, Ford LG, Parnes HL, Minasian LM, Gaziano JM, Hartline JA, Parsons JK, Bearden JD, Crawford ED, Goodman GE, Claudio J, Winquist E, Cook ED, Karp DD, Walther P, Lieber MM, Kristal AR, Darke AK, Arnold KB, Ganz PA, Santella RM, Albanes D, Taylor PR, Probstfield JL, Jagpal TJ, Crowley JJ, Meyskens FL Jr, Baker LH, Coltman CA Jr (2009) Effect of selenium and vitamin E on risk of prostate cancer and other cancers: the Selenium and Vitamin E Cancer Prevention Trial (SELECT). JAMA 301:39–51
10. El-Bayoumy K (2009) The negative results of the SELECT study do not necessarily discredit the selenium-cancer prevention hypothesis. Nutr Cancer 61:285–286
11. Ip C (1998) Lessons from basic research in selenium and cancer prevention. J Nutr 128:1845–1854
12. Ravn-Haren G, Bugel S, Krath BN, Hoac T, Stagsted J, Jorgensen K, Bresson JR, Larsen EH, Dragsted LO (2008) A short-term intervention trial with selenate, selenium-enriched yeast and selenium-enriched milk: effects on oxidative defence regulation. Br J Nutr 99:883–892
13. Zhao H, Brooks JD (2007) Selenomethionine induced transcriptional programs in human prostate cancer cells. J Urol 177:743–750
14. Cao TM, Hua FY, Xu CM, Han BS, Dong H, Zuo L, Wang X, Yang Y, Pan HZ, Zhang ZN (2006) Distinct effects of different concentrations of sodium selenite on apoptosis, cell cycle, and gene expression profile in acute promyeloytic leukemia-derived NB4 cells. Ann Hematol 85:434–442
15. Hu H, Jiang C, Ip C, Rustum YM, Lu J (2005) Methylseleninic acid potentiates apoptosis induced by chemotherapeutic drugs in androgen-independent prostate cancer cells. Clin Cancer Res 11:2379–2388

16. Sanmartín C, Plano D, Palop JA (2008) Selenium compounds and apoptotic modulation: a new perspective in cancer therapy. Mini Rev Med Chem 8:1020–1031
17. Wang Z, Hu H, Li G, Lee HJ, Jiang C, Kim SH, Lu J (2008) Methylseleninic acid inhibits microvascular endothelial G_1 cell cycle progression and decreases tumor microvessel density. Int J Cancer 122:15–24
18. Corcoran NM, Najdovska M, Costello AJ (2004) Inorganic selenium retards progression of experimental hormone refractory prostate cancer. J Urol 171:907–910
19. Plano D, Sanmartín C, Moreno E, Prior C, Calvo A, Palop JA (2007) Novel potent organoselenium compounds as cytotoxic agents in prostate cancer cells. Bioorg Med Chem Lett 17:6853–6859
20. Ibáñez E, Plano D, Font M, Calvo P, Prior C, Palop JA, Sanmartín C (2011) Synthesis and antiproliferative activity of novel symmetrical alkylthio- and alkylselenocarbamates. Eur J Med Chem 46:265–274
21. Moreno D, Plano D, Baquedano Y, Jiménez-Ruiz A, Palop JA, Sanmartín C (2011) Antileishmanial activity of imidothiocarbamates and imidoselenocarbamates. Parasitol Res 108:233–239
22. Sanmartín C, Plano D, Domínguez E, Font M, Calvo A, Prior C, Encío I, Palop JA (2009) Synthesis and pharmacological screening of several aroyl and heteroaroyl selenylacetic acid derivatives as cytotoxic and antiproliferative agents. Molecules 14:3313–3338
23. Plano D, Baquedano Y, Ibáñez E, Jiménez I, Palop JA, Spallhoz J, Sanmartín C (2010) Antioxidant-prooxidant properties of a new organoselenium compound library. Molecules 15:7292–7312
24. Plano D, Moreno E, Font M, Encío I, Palop JA, Sanmartín C (2010) Synthesis and in vitro anticancer activities of some selenadiazole derivatives. Arch Pharm Chem Life Sci 10:680–691
25. Sheldrick GM (1997) SADABS: program for empirical absorption corrections. University of Göttingen, Göttingen, Germany
26. Sheldrick GM (2008) A short history of SHELX. Acta Crystallogr A 64:112–122
27. Li Y, Pan J, Li JL, Lee JH, Tunkey C, Saraf K, Garbe JC, Whitley MZ, Jelinsky SA, Stampfer MR, Haney SA (2007) Transcriptional changes associated with breast cancer occur as normal human mammary epithelial cells overcome senescence barriers and become immortalized. Mol Cancer 6:7
28. Mosmann T (1983) Rapid colorimetric assay for cellular growth and survival: application to proliferation and cytotoxicity assays. J Immunol Methods 65:55–63